IEEE Access
Multidisciplinary : Rapid Review : Open Access Journal

Received September 3, 2020, accepted September 18, 2020, date of publication October 8, 2020, date of current version October 22, 2020.

Digital Object Identifier 10.1109/ACCESS.2020.3029602

Intelligent Handover Prediction Based on Locational Priority With Zero Scanning for the Internet of Underwater Things

SEOKHYEON PARK AND OHYUN JO, (Member, IEEE)
Department of Computer Science, Chungbuk National University, Cheongju 28644, South Korea
Corresponding author: Ohyun Jo (ohyunjo@chungbuk.ac.kr)

This research was a part of the project entitled 'Development of Distributed Underwater Monitoring and Control Networks', funded by the Ministry of Oceans and Fisheries, South Korea. In part, this research was supported by Basic Science Research Program through the National Research Foundation of Korea (NRF) funded by the Ministry of Education (2020R1A6A1A12047945). This research was also supported by the MSIT (Ministry of Science and ICT), Korea, under the Grand Information Technology Research Center support program (IITP-2020-0-01462) supervised by the IITP (Institute for Information & communications Technology Planning & Evaluation).

ABSTRACT It is becoming clear that the maritime industry is expected to see considerable growth over the coming years, and the Internet of Underwater Things (IoUT) could have an essential role to play in its technological development. In this regard, because batteries are the main power source in underwater environments, there is a clear need to minimize the consumption of energy. In addition, underwater links that make use of acoustic soundwaves can cause relatively long propagation delays. In our proposed scheme, we focus on the initial connection procedure between sensor nodes and underwater base stations to tackle these environmental problems, in which the former estimates the signal strength of the latter. From local information measured during the initial network entry phase, underwater sensor nodes determine locational priority of candidate targets, but do not scan or measure the signal strength of other neighbouring underwater base stations as a means of keeping the power consumption to an absolute minimum. This can be considered an appropriate scenario for use in severely battery-limited environments such as IoUT. Based on analysis using machine learning, we obtain meaningful clues regarding the procedure for handover prediction without channel measurement. By removing the overhead from the channel measurement, the power consumption of the underwater things can be minimized. Two different methods of deciding on handover priority are suggested and analysed mathematically. The performance of each method is evaluated through intensive system-level simulations and compared to that of a more conventional scheme.

INDEX TERMS Locational priority, machine learning, handover prediction.

I. INTRODUCTION

With the passage of time, more and more electronic devices have been devised to adopt wireless communication systems [1], [2]. Because there is less restriction on the mobility of nodes in wireless than in wired communications, the needs of wireless devices are continuing to increase, as is their functionality. The development of industries using wireless communication systems like IoT, smart vehicles or mobile technology implies the adoption of wireless systems in diverse areas. The demand for wireless communication systems is also increasing for underwater applications [3].

The associate editor coordinating the review of this manuscript and approving it for publication was Mubashir Husain Rehmani.

For example, the adoption of standards for underwater communications and underwater observation webs by the North Atlantic Treaty Organization (NATO) has led to various underwater applications by organizations such as Ocean Networks Canada, the Ocean Observations Initiative, and Smart Bay. The so-called Internet of Underwater Things (IoUT) can be used in many different areas, for example, national defence, marine disasters, fisheries, observations for marine resources, diver communications, or marine rescue [4]–[6].

In all these areas, there are many cases where mobility is required. Moreover, sensor nodes may possibly be forced by tides or other environmental drivers [7]–[10], and in this regard, handover methods might be required in IoUT networks [11], [12].

Since the IoUT network mostly makes use of acoustic waves, it is characterized by velocities of around 1500m/s, which are much slower than that of microwaves. In addition, it is vulnerable to noises made both on the ocean surface and at depth. It also suffers from numerous restrictions such as multipath fading, slow data transmission, substantial propagation losses, limited energy when using batteries, and severe hidden-node problems [13]–[17]. Therefore, it is only barely possible to apply existing conventional handover methods to IoUT networks [18]–[20]. It is generally necessary to measure locations or signal strengths by transmitting measurement reference signals between sensor nodes and a number of base stations. However, this causes significant performance degradation in IoUT networks. Furthermore, long propagation delays mean that the sensor node may be in a different location by the time the channel measurement is completed. Underwater environments have many limitations that affect the tasks undertaken by humans, and underwater devices have communication functions in the form of non-power and Lightweight sensor nodes [21]–[23].

In this paper, we propose a handover priority decision method that is applicable to IoUT networks and may be used to solve the aforementioned problems based on locational probabilities and machine learning with zero scanning. Two alternatives are discussed and evaluated, which uses only the signal information created in the initial network entry process between base stations and sensor nodes to remove measurement overhead. Sensor nodes never perform neighbouring cell measurement after network entry procedures. This approach does not consume additional energy to measure all candidate neighbouring cells because it uses saved signal information with no need for any measurements. The handover procedure best suited to IoUT networks is proposed and evaluated at the system level.

II. RELATED WORK

A. BACKGROUND

In the case of IoUT, by the environmental specificity, on-surface wireless communication systems cannot be applied [13]–[17]. Therefore, many different IoUT models that fit the underwater characteristics have been suggested [24]–[29]. The method tuned to fit the underwater environment was suggested based on the IEEE 802.11 protocol used on the surfaces [6], [28]. Experiments are conducted with many different media like RF, visible light, etc., mainly the models using acoustic wave communications were many because they had fewer restrictions on communication distance in underwater environments [13]–[17].

1) PROBLEM STATEMENT

IoUT has many practical problems due to environmental reasons. First of all, there is an energy problem. When communication is conducted under deep water, consistent energy supply is hardly possible. That means, once a battery equipped node is installed, its maintenance is almost impossible. Thus, for underwater wireless networks, it must be designed to be used for as long as possible with minimum energy usage after installation. This is the most critical issue of the underwater acoustic wave wireless networks, and many challenges to solve this have been conducted [3], [20], [36]. Moreover, acoustic wave is very slow with the speed of 1500m/s underwater, and the data transmission speed is very restricted, so there are many difficulties with large data transmission [4], [37], [46].

B. RELATED WORK

1) RESEARCHES ABOUT THE PREVIOUS UNDERWATER HANDOVER METHODS AND ITS PROBLEMS

In [38] suggests an ocean current prediction method through machine learning. It makes the prediction model by collecting marine data and predicts the movement of nodes that move passively by the tides at the underwater environments. The high accuracy of the machine learning model supports handover through the predicted movements of the nodes and motivates this work.

Handover methods for underwater visual light Ad-hoc diver networks were discussed in [39]. In this work, if a diver gets out of the communication range while communicating with other divers using visual light, the handover is performed by using other diver(diver bridge) between transmitter and receiver. This result has presented about the handover protocols, yet it is just a suggestion of the concepts, there is no experiment or investigation. Also, since it uses the visual light, there is a restriction for the distance between nodes.

To the best of the our knowledge, handover technology using acoustic wave in underwater wireless networks, the methods suggested in [38] and [45] are the known options. The lack of previous researches or the standards leads to unsystematized design in future researches because there is not sufficient reference.

Thus, this paper suggests a new concept that has not been mentioned before. It would be helpful for many underwater handover researches in the future. In addition, this research possibly can be applied to the practical IoUT network that we are currently working for a huge project supported by Korean government [40]–[44]. Numerous research institutes, universities, and global IT companies such as SK Telecom are involved in this on-going project for commercialization of IoUT applications [47], [48]. Actually, the testbeds designed in this project are on the level of the practical test.

2) PREDICTION OF UNDERWATER SENSOR LOCATION WITH ZERO CHANNEL MEASUREMENT

The proposed method is intended to minimize the consumption of energy by removing the need for channel measurement. Before considering the handover procedure, we first needed to address the possibility and feasibility of handover methods without channel measurement in IoUT environments.

While it may be impossible to predict the position of sensor nodes without channel monitoring due to the uncertainties of mobile users on land, using information on ocean current prediction based on machine learning algorithms, the movement of underwater sensor nodes may be predictable in IoUT environments [38].

The prediction of node location for IoUT is based on ocean currents. If we assume that sensor nodes are lightweight and move passively with currents, models for predicting ocean currents may help simulate the mobility of underwater sensor nodes without the need for channel measurement.

We also used machine learning technologies for evaluation purposes, and to that end data were obtained for the real underwater environment off the southeastern coast of the Korean peninsula, and were used for training and validation. An ocean current prediction model was thus trained using a variety of sea information data with the aim of predicting the movements of sensor nodes.

The data used for learning is gathered by collaboration with Korea Hydrographic and Oceanographic Agency, and it is actual data collected at the location pointed in Fig. 1.

FIGURE 1. The location for the ocean data collection from the South Sea of Korea.

The training set includes recent measured data on surface velocity, surface flow (direction), water temperature, and salinity for a four period at 30-minute intervals.

We devised 5 machine learning models, namely MLR (Multiple Linear Regression), MLP (Multi-Layer Perceptron), SVM (Support Vector Machine), DTC (Decision Tree Classification), and KNN (K-Nearest Neighbors). All of them produce highly accurate predictions of ocean currents for estimating the mobility of underwater sensor nodes.

Fig. 2 shows the prediction accuracy of the 5 machine learning models. In the present study we used various different machine learning models to make the predictions. The term 'Rank' is herein defined as the number of candidates for which an accurate target handover cell can be determined.

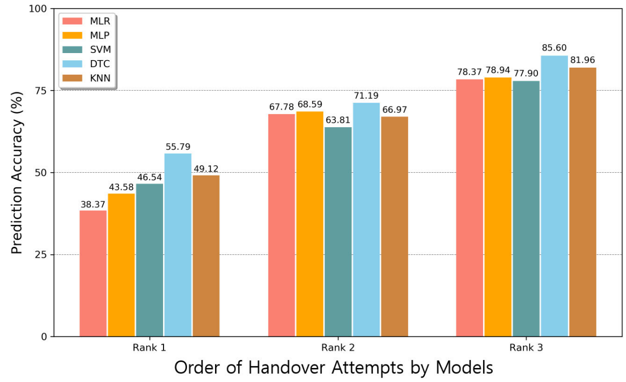

FIGURE 2. Prediction accuracy of the underwater sensor nodes using many machine learning models.

In other words, for a Rank n, the machine learning model predicts n candidate target cells. The prediction accuracy in Fig. 2 is defined as the probability that the correct target cell in practice is contained in n candidate target cells as determined by the machine learning models.

Figure 2 shows that the prediction accuracy can be more than 80% if we adopt machine learning models to predict the mobility of sensor nodes in underwater environments. A total of 6 base stations are located around the central base station in the suggested sea current prediction model environment, meaning that the model can predict the direction within a rank of up to 6. For the prediction results, we show the accuracy of the proposed model for Rank 1, 2, and 3. The success of these predictions means that handover can be applied without channel monitoring.

In this paper, we describe the prediction of the mobility of sensor nodes under these conditions. Two methods are proposed for the handover procedure. The first makes use of candidate counts, and the second uses the difference in signal strength at the point of initial network entry.

III. PROPOSED UNDERWATER HANDOVER PROCEDURE WITH ZERO SCANNING

A. UNDERWATER CHANNEL MODELS

For the underwater wireless communications, many different channel models were suggested depending on the media while taking into account the various environmental effects such as signal decrease, antenna radiation pattern, and multi-thread fading following the sea surface.

In [30] handles the factors which are to be considered at the underwater RF communications. It claims that the wireless sensor network is settable at the underwater environment through the mathematical analysis of various factors like electromagnetic properties of water, transition frequency, reflections, channel characteristics, multipath. This research, however, raises many problems like path loss due to a decrease, or necessity of remodeling RF communication equipment.

In [31] and [32], it shows the use of high-frequency RF communications. And [31] shows 4G transmitter-receivers

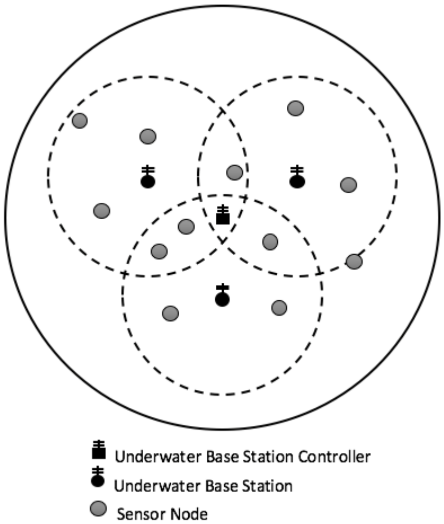

FIGURE 3. System model of internet of underwater things.

are usable for underwater communications, tranceivers using insulator were considered in [32]. However, they also show that underwater RF communications still have many limits when it comes to long-distance communications.

Communication channel modeling method was discussed in [33]. And In [34], the long-distance underwater visual light wireless communication channel models are suggested and analyzed. They also show that the visual light communications have difficulties due to absorption and scattering.

The problems of the underwater acoustic wave networks based on acoustic wave modems and their environmental characteristics are discussed in [3]. The research result applying OFDM to underwater wireless acoustic wave channels is presented in [35].

B. SYSTEM MODEL OF UNDERWATER HANDOVER SCENARIOS

Before discussing handover technologies for IoUT networks, we present the system model of IoUT considered in this work.

Although many kinds of model are possible, we present a practical system model composed of UBSCs (Underwater Base Station Controllers), UBSs (Underwater Base Stations), and the SN (Sensor Node). This system model is designed and implemented for commercial IoUT applications in South Korea [40]–[44].

Numerous research institutes, universities, and global IT companies including SK Telecom have been involved in this large research project for several years. In this practical system model, SNs collect data from marine environments, such as temperature, current speed, and salinity. They then deliver this information to the connected UBS. The UBSs manage a number of sensor nodes within the their communication range, receive the collected data from their sensor nodes, and combine and send them to the UBSC. The UBSC transfers the collected data to other networks on land for connection to the Internet. Our IoUT network structure is shown in Fig 3. The solid line shows the coverage of UBSCs, and the dotted line shows the coverage of UBSs. The UBSCs control the UBSs and the UBSs control the sensor nodes within their area of coverage. The detailed structure is one where the UBSC takes charge of 3 UBSs. The operational scenario of our practical system model takes place via the following procedures for managing IoUT networks.

1) Deploying UBSCs, UBSs, and sensor nodes
2) Searching for connection between UBSCs and UBSs, and between UBSs and sensor nodes, and the attempt to connect
3) Completion of searching and setting system environments
4) Entering data transmission phase

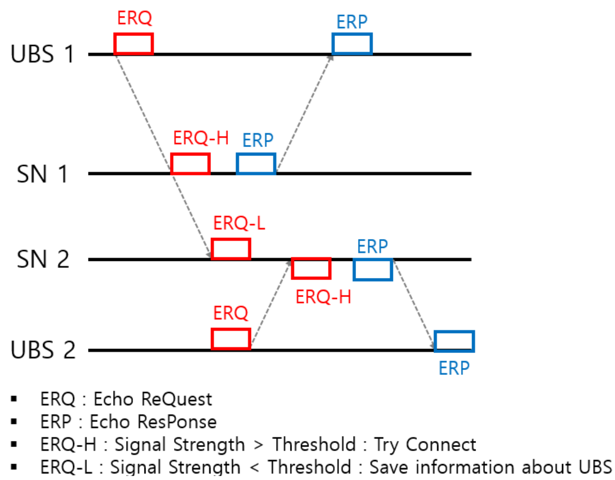

FIGURE 4. Example of control packet transmissions for searching and connecting method in system.

Fig. 4 shows the procedure for search and connection between 2 UBS's and 2 SNs. UBS transmits ERQ(Echo ReQuest) message to SN within the range. Then the SN measures the signal strength of the received packet, and compares it with the predefined threshold value. If the signal strength is stronger than the threshold, it attempts to connect with UBS by sending ERP(Echo ResPonse) message. If not, it saves the information of the UBS and waits for the signal from other UBSs. In practical situations, this process is performed several times to solve the problems of lost packets. This method is conducted at the initial connection level, and once they are connected, it moves on to the data transmission phase. The details are in Section III.

C. HANDOVER TRIGGER CONDITION

In this section, we explain the handover trigger condition for the underwater sensor nodes. On land, handover is widely used for mobile devices. Mobile devices in outdoor communication systems measure the signal strength of neighbouring cells periodically before calculating the most appropriate time for handover and the target neighbour cell. However, since energy is restricted in IoUT networks, the handover trigger condition must be appropriate for underwater sensor nodes, as follows

Algorithm 1 Handover Trigger Procedure

```
if transfer_data() then
    transfer_time[].append(transfer_timer())
    rtt_timer()
    transfer_timer()
end if
if receive_ack() then
    rtt_time[].append(rtt_timer())
    sn_dist[].append(calc_rtt(rtt_time[]))
    max_timer = max(transfer_time[])
    average_speed = average(sn_dist[]) / average(rtt_time[])
    deadtime = (max_range − sn_dist[LAST]) / average_speed
    if deadtime < max_timer then
        handover_request()
    end if
end if
```

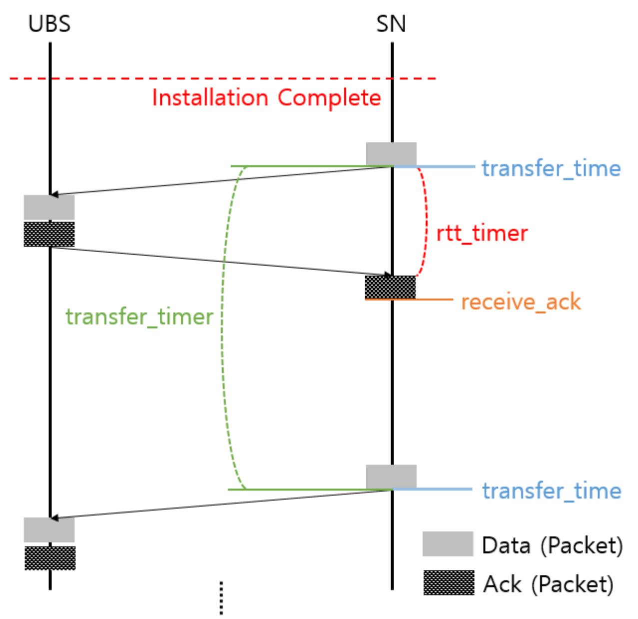

FIGURE 5. Description of handover trigger parameter using packet flow procedure.

Algorithm 1 contains a listing of how the handover trigger procedure works, and Fig. 5 gives a brief overview of the parameter about the handover trigger procedure. Table 1 shows the parameter information defined in the system specification. When a sensor node sends data to its UBS, two types of timing parameter are measured, namely the time to receive ACK and the time gap between receipt of the previous data and receipt of the current data. The time taken is saved into an array structure called transfer_time. Afterwards, when the ACK packet has been transmitted from the UBS,

TABLE 1. Handover trigger procedure parameter.

Parameter	Function
transfer_timer()	Measure time between last data transfer and current data transfer
transfer_time[]	A collection of time measured by transfer_time()
rtt_timer()	Measure time between data transfer and ack received
rtt_time[]	A collection of time measured by rtt_timer()
calc_rtt()	Calculated distance between sensor node and UBS using rtt_time[]
sn_dist[]	A collection of distance calculated by calc_rtt()
max_timer	The largest value of transfer_time[] element (Longest waiting time)
average_speed	Sensor node average rate so far
sn_dist[LAST]	Sensor node location information measured by latest time
max_range	The maximum radio reception distance of the base UBS
deadtime	Value of threshold for handover trigger condition, When a sensor node moves at a measured average speed(average_speed), The time it takes to the maximum radio reception distance of the UBS
handover_request()	Handover request function

the distance between the sensor node and the connected UBS is calculated using RTT(Round Trip Time). To predict when the sensor node moves out of range of the connected UBS, the longest time in the array transfer_time is retained. Based on the measured data, the average speed and the deadtime are also calculated as shown in the the pseudo code. Handover is attempted when the deadtime is shorter than max_timer. Due to the characteristics of IoUT networks, data transmission is erratic, and it is hard to determine the exact time at which the sensor node escapes out of the communication range. By considering the underwater characteristics, an average speed of the sensor node per unit time is used. Using the longest transfer_time and the longest deadtime, considered as the last data transmission before the sensor node escapes from the range of the connected UBS, the request for handover is sent to the UBS.

IV. PROPOSED APPROACH

A. PROPOSED UNDERWATER HANDOVER PROCEDURES

Two locational priority-based handover methods are proposed in this section. From the initial network entry processes between the sensor nodes and the UBSs, messages are passed, and these methods are used to measure the signal strength of the signalling packets during the initial connection procedure for the first and the last. These methods can prevent additional energy consumption by using information on signal strength obtained during the essential initial procedure.

IoUT networks can use this policy to reduce energy consumption as much as possible. Two methods are proposed, discussed, and evaluated, namely UCC (Using the Candidate UBS Counts) and UDSS (Using the Difference of Signal Strength).

1) UCC METHOD USING CANDIDATE UBS COUNTS

Under UCC, the signal strength of the data transmitted during the initial search and connection process is measured, saved, and noted. This process is essential for the connection between sensor nodes and UBSs. The strength of the signal is measured using a sensor node. If the signal strength of a candidate UBS is larger than the threshold, the UBS is enrolled at the sensor node. Given the number of enrolled candidate UBSs, it is then possible to guess the location of the sensor node, which can be calculated using the well known triangulation method [45].

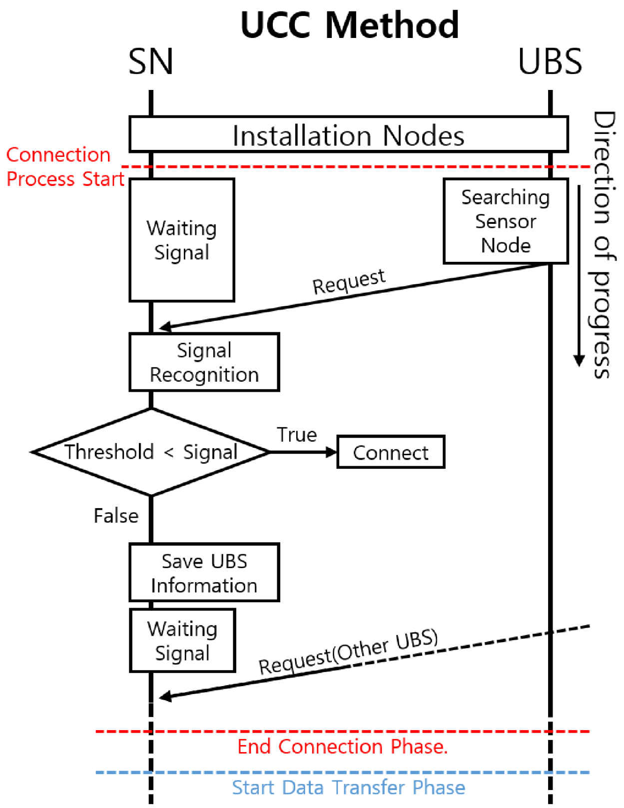

FIGURE 6. Flowchart of UCC method using candidate UBS counts.

Algorithm 2 UBS - Sensor Node Connection Process and Candidate Base Station Registration Process

```
Waiting_Signal()
UBS_Signal_Recognition()
if Threshold < Signal then
    Connection_UBS()
else
    Save_UBS_Infomation()
    Waiting_Another_Signal()
end if
```

The process of connection between the sensor node and UBSs for enrolling candidate UBSs is presented in Fig.6. And Algorithm 2 shows process of connection using pseudocode.

During the process of connection between the UBS and the sensor node, the sensor node measures the signal strength, and if the signal strength does not exceed the threshold, it deems the UBS to be a candidate without connecting with it. After this, when the sensor node receives signals from another UBS, it measures the signal strength and checks whether it exceeds the threshold. This process continues until the sensor node finds a signal that exceeds the threshold. Thus, information about all the other UBSs that had a lower received signal strength than the threshold is saved.

If the sensor node fulfills the condition of the handover trigger, handover priority is decided using the saved information about candidate UBSs without measuring any neighbouring channel or scanning any neighbouring cells. We thus describe the proposed handover methods as featuring zero neighbouring channel scanning and discovery. If the UBS that meets the condition is not detected during the process of searching and connection, the sensor node tries to connect with the one with the strongest signal using saved information about candidate UBSs. The signal strength can be considered proportional to the distance it moves in an ideal situation without refraction, interference, or resistance.

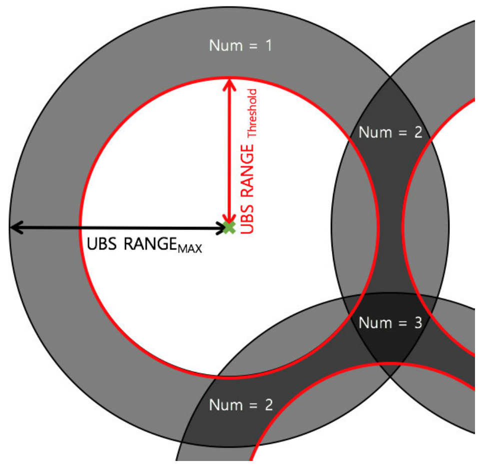

FIGURE 7. Number of candidate base stations generated for a given threshold of underwater base stations and a maximum radio reach.

Assuming that signal strength is proportional to distance, the number of candidate UBSs calculated within the threshold can be determined as shown in Fig 7. Around the centre of the circle in which the UBS is located, there are as many candidate UBSs as the number of overlaps of UBS $\mathrm{RANGE}_{\mathrm{MAX}}$ and UBS $\mathrm{RANGE}_{\mathrm{Treshold}}$. Using the number of candidate UBSs, the approximate location of the sensor node can be estimated, and the handover target cell priority can then be decided. The whole process is presented in Algorithm 3.

In order to discuss the procedure for determining handover priority using the number of candidate UBSs, definitions of internal and external UBSs are required. Internal UBSs are defined as those that are connected to their UBSC and which exist inside its coverage. External UBSs are regarded as those UBSs that do not exist inside the coverage of the UBSC. We now describe three possible cases.

a: CASE 1: CANDIDATE UBS COUNT IS 1

When the sensor nodes are moving out of range of the connected UBS, it is considered that they could possibly

Algorithm 3 Determining Handover Priorities Based on the Number of Candidate Underwater Base Stations

```
Moving_Node_Detection_Mode()
if Node_Out_of_Range() then
    Handover_Request()
    if Candidate_UBS_Count() == 1 then
        Nearest external base station connection
    end if
    if Candidate_UBS_Count() == 2 then
        Connect with candidate UBS
        (except connected UBS)
    end if
    if Candidate_UBS_Count() == 3 then
        Connect in strongest candidate UBS
        (except connected UBS)
    end if
else
    Moving_Node_Detection_Mode()
end if
```

head in the direction of the external UBS. Thus, handover is attempted for the closest of the external UBSs.

b: CASE 2: CANDIDATE UBS COUNT IS 2

When the sensor nodes are moving out of range of the connected UBS, handover is attempted with one of the internal UBSs other than the currently connected one. If the trial of the handover with the candidate UBS fails, connection is attempted with other UBSs not identified as candidates.

c: CASE 3: CANDIDATE UBS COUNT IS 3

Handover is attempted with the UBS with the strongest signal among the candidate UBSs other than the currently connected UBS. If it fails, connection is attempted with the next strongest UBS.

2) UDSS METHOD USING DIFFERENCE OF SIGNAL STRENGTH OF EACH UBS

The UDSS (Using the Difference of Signal Strength) method works by measuring and using the strength of the signal transmitted from all the UBSs in the range of the sensor node. Because it works by measuring the signal strength of all UBSs, the sensor node should know the number of UBSs that surround it. The sensor node saves the signal strength from the UBSs. Consequently, the handover priority is determined from the difference of signal strength.

Fig. 8 shows the IoUT connection procedure for the UDSS method. And Algorithm 4 shows UBS connection process.

We explain the prediction procedure for the location of the sensor node using the difference in signal strength from the UBSs. Fig. 9 shows the position of the sensor nodes according to signal strength difference. We assume that the sensor node is connected to UBS_A with the strongest signal. In this case, the location of the sensor node predicted from the difference in signal strength can be classified into 3 regions.

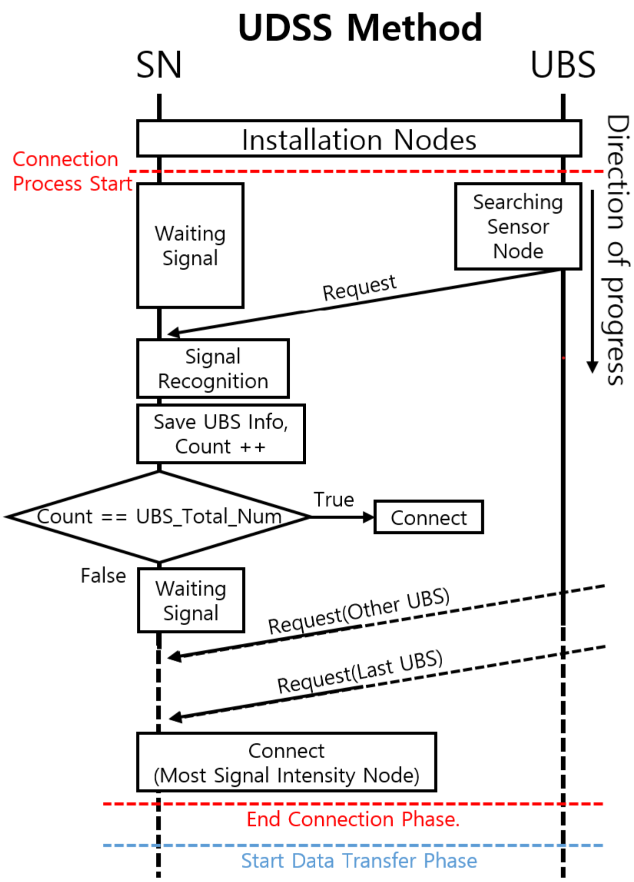

FIGURE 8. Flowchart of UDSS method using signal strength difference.

Algorithm 4 Underwater Base Station Connection Process

```
Waiting_Signal()
UBS_Signal_Recognition()
Save_UBS_Infomation()
Count++
if Count == UBS_Total_Num() then
    Connection_UBS(MAX(Signal))
else
    Waiting_Another_Signal()
end if
```

① $\xi_{UBS_B} \approx \xi_{UBS_C}$ && $\xi_{UBS_A} \gg \xi_{UBS_B}$ && $\xi_{UBS_A} \gg \xi_{UBS_C}$

② $[\xi_{UBS_A} \approx \xi_{UBS_B}$ && $\xi_{UBS_B} \gg \xi_{UBS_C}]$ || $[\xi_{UBS_A} \approx \xi_{UBS_C}$ && $\xi_{UBS_B} \ll \xi_{UBS_C}]$

③ $\xi_{UBS_A} \approx \xi_{UBS_B} \approx \xi_{UBS_C}$

Here, ξ_{UBS_A}, ξ_{UBS_B}, and ξ_{UBS_C} denote the signal strength of base stations *UBS_A*, *UBS_B*, and *UBS_C*, respectively. The sensor node can be assumed to be located in region ① when the signal from *UBS_B* and *C* is weak (but the *B* and *C* signal strengths are similar) and the signal from *UBS_A* is strong.

In region ②, two conditions are possible. In the first, the signal strengths of *UBS_A* and *UBS_B* are similar and the signal from *UBS_C* is weak. In the second, the signal

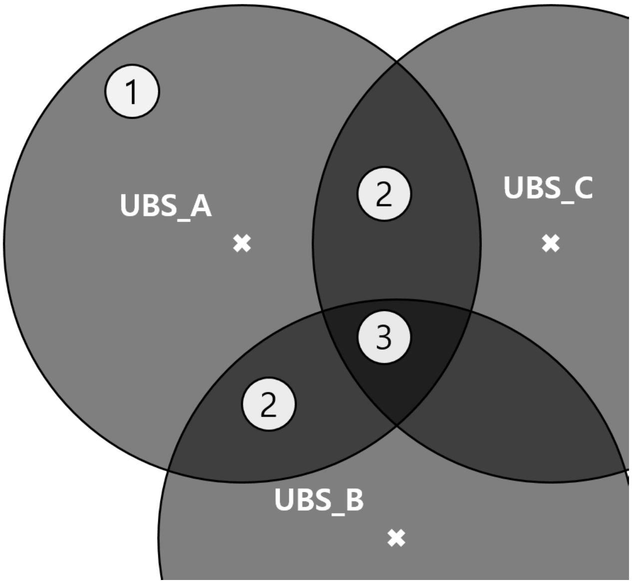

FIGURE 9. Position of sensor nodes in IoUT network structure according to difference in signal strength.

strengths of UBS_A and UBS_C are similar and the signal from UBS_B is weak.

The sensor node can be assumed to be located in region ③ when the strengths of the signals from all the UBSs are similar. If the sensor node connected to UBS_A is located in region ② and is moving far away from the connected base station, handover is attempted with UBS_B(or UBS_C), which is the next strongest UBS. If handover fails, it attempts to connect with the next strongest UBS. A sensor node located in region ③ also attempts handover in order of signal strength. In the location of ①, handover is not attempted with the internal UBS.

Similar to Case 1 of the UCC method, by assuming that the sensor nodes are most likely to be heading in the direction of the external UBS, handover is requested first with the closest external UBS.

B. ANALYSIS AND PERFORMANCE EVALUATION

In this section, a probabilistic rationale and a geometric analysis are proposed to show that the sensor nodes may select a proper target cell with zero neighbour scanning or neighbour discovery with a fairly high probability by using the proposed methods in a real situation. Also, we observe how the frequency of network crashes varies according to the handover success probability. Table 2 shows the parameter information used in analysis Fig. [45].

For the geometric analysis, it is assumed that a sensor node A(SN_A) is connected to a certain base station noted by UBS_A. The sensor node can be considered to be located in the grey-coloured area when the candidate UBS count is 1 or when the signal strength from UBS_A is the highest, and the signals from the others are relatively weak.

TABLE 2. Formulation paramete for analysis and performance evaluation [45].

Parameter	Function
A_{len}	Length of line A
B_{len}	Length of line B
C_{len}	Length of line C
D_{len}	Length of line D
E_{len}	Length of line E
F_{len}	Length of line F
G_{len}	Length of line G
α	Angle between line A and line C
β	Angle between line C and line D
γ	Angle between line D and line F
SN_A_{escape}	Escape probability from the current UBS
H_{slope}	The slope for a line H
I_{slope}	The slope for a line I
J_{slope}	The slope for a line J
K_{slope}	The slope for a line K
δ	Angle between horizontal line and line I
ε	Angle between horizontal line and line K
SN_B_p	The probability that the sensor node B is heading to the internal base station without leaving the external base station

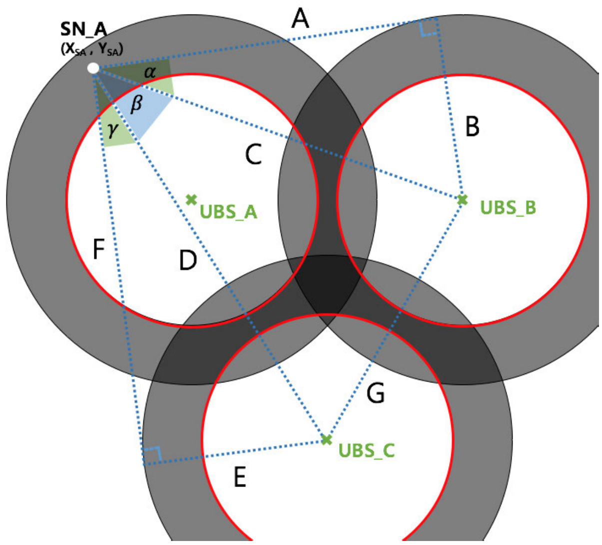

FIGURE 10. The probability that a moving sensor node will face an external UBS.

Assuming that the sum of the angles α, β, γ implies that the heading is towards the internal UBSs, the probability that the heading of the sensor node will get away from the UBS for given α, β, γ can be calculated as follows. In this formulation, A_{len}, B_{len}, C_{len}, D_{len}, E_{len}, F_{len}, G_{len} are defined as the lengths of lines A, B, C, D, E, F and G in Fig. 10.

$$\alpha = \arccos(A_{len}/C_{len}) \tag{1}$$
$$\beta = (C^2_{len} + D^2_{len} + G^2_{len})/2 * C_{len} * D_{len} \tag{2}$$
$$\gamma = \arccos(F_{len}/D_{len}) \tag{3}$$

The angle of the external UBS direction can be obtained by subtracting the internal UBS angle from 360 degrees. Thus, the probability that the sensor node will escape to an external UBS is formulated as follows. In this formulation, SN_A_{escape}

denotes the escape probability from the current UBS.

$$SN\_A_{escape} = (360 - (\alpha + \beta + \gamma))/360 \quad (4)$$

The induced formula above, the possibility that a sensor node would leave to an external base station is calculated as 77% maximum [45].

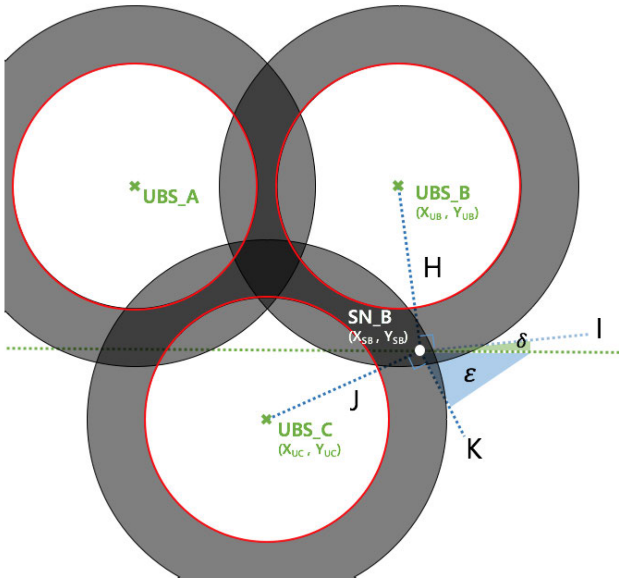

FIGURE 11. **Probability of sensor node heading for candidate base station.**

In the case of Fig. 11 which shows that SN_B is connected to UBS_B, The sensor node can be considered to be located in the dark grey area when the candidate UBS count is 2 or when the signal strengths from UBS_B and UBS_C are similar while the signal from UBS_A is the weakest. In this situation, the sum of the angles δ, ε is the angle of escape to the direction of the external UBSs. Angle δ, ε can be calculated from the slopes of lines I and K, relative to the lines H and J, respectively.

In the following formulations, X_{UB}, Y_{UB} denote the distances of the X-axis and Y-axis from UBS_B, and X_{UC}, Y_{UC} denote the distances of the X-axis and Y-axis from UBS_C in Fig. 11. X_{SB}, Y_{SB} indicate the distances of the X-axis and Y-axis from SN_B.

$$H_{slope} = (Y_{UB} - Y_{SB})/(X_{UB} - X_{SB}) \quad (5)$$
$$J_{slope} = (Y_{UC} - Y_{SB})/(X_{UC} - X_{SB}) \quad (6)$$
$$I_{slope} = -(1/H_{slope}) \quad (7)$$
$$K_{slope} = -(1/J_{slope}) \quad (8)$$

By adapting the reverse tangent to I_{slope} and K_{slope}, the value of the angles δ, ε can be calculated.

$$\delta = \arctan(I_{slope}) \quad (9)$$
$$\varepsilon = \arctan(K_{slope}) \quad (10)$$

"SN_B_p" is defined as the probability that the sensor node B is heading to the internal base station without leaving the external base station, and can be obtained as follows.

$$SN\_B_p = (180 - (\delta + \varepsilon))/180 \quad (11)$$

The value of SN_B_p may change according to the initial location of the sensor node, but in most situations the sensor node heads to the candidate UBS with the highest probability.

By the induced formula above, the possibility that a sensor node would move toward the other potential base station within the range is calculated as 82%. This means that a sensor node would head to the internal candidate base stations at most of the locations.

In particular, the sensor node can be considered to be located at the centre of the UBSC when the candidate UBS count is 3 or when signal strengths from all the UBSs are similar. In this situation, sensor nodes are most likely to head to an internal UBS no matter what direction it moves. In this regard, the handover target cell can be determined among the internal UBSs.

We performed an intensive system level simulation together with mathematical and geometric modelling to show the accuracy of the proposed handover prediction model. The tests were conducted assuming that the nodes connected to the UBS are moving far and in an inconstant direction in the aforementioned three cases in Fig. 3 and Fig. 7.

V. EXPERIMENTAL SETUP

This research suggests a handover method which prevents additional energy usage by using inevitably collected information. Also, it conducted probabilistic, mathematical, and geometric investigations about the suggested method. However, it is necessary to check if the method can work in real environments. This chapter discusses the environments, parameters, and the results of the system level simulations for these verifications.

A. SIMULATION ENVIRONMENT AND PARAMETER

The system level simulator designed and implemented by using Python. Additionally we used open-library such as Numpy and Matplotlib for implementation of the simulations. The composition of the base stations used in the practical experiment is shown in Fig. 12.

In this simulation, one UBSC contains 3 UBSs, and 3 UBSCs(9 UBS's) were composed in total. The deployment of the test scenario is corroborated with the specification of the real IoUT network which is implemented in the aforementioned project supported by Korean government. The coordinates and the simulation parameters of the UBSCs and the UBS's are as described on Fig. 13.

Two types of experiments are conducted, the first experiment was about whether the sensor nodes move like the suggested method in practice, and the second one was about the affect of the incorrect handover prediction to the IoUT networks.

Fig. 14 shows the simulation progress about the movement of sensor nodes. In this simulation, sensor nodes are located on random coordinates and moved to random directions from

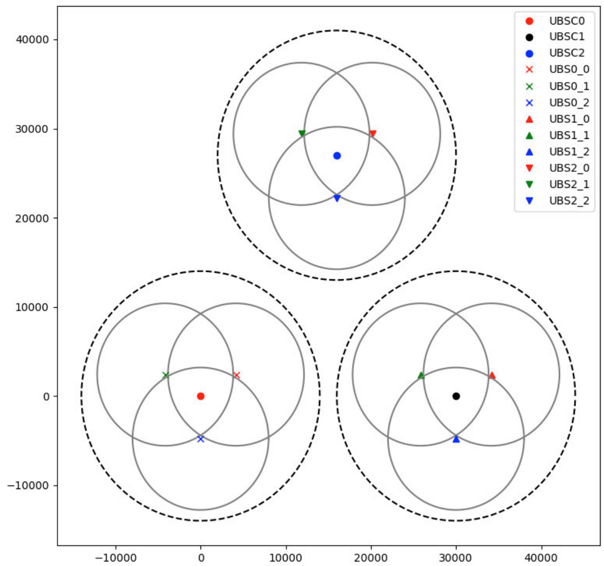

FIGURE 12. Handover simulation environment and nodes configuration.

Parameters

Node Mobility Simulation

Node	X-axis(m)	Y-axis(m)
UBSC0	0	0
UBSC1	30000	0
UBSC2	16000	27000
UBS0_0	4156	2400
UBS0_1	-4156	2400
UBS0_2	0	-4800
UBS1_0	34156	2400
UBS1_1	25843	2400
UBS1_2	30000	-4800
UBS2_0	20156	29400
UBS2_1	11843	29400
UBS2_2	16000	22200

Collision Rate Simulation

Acoustic wave	1500 m/s
UBSC Range	10000 m
UBS Range	5000 m
Installed Node	10
Added Node (Max)	5
Random Back Off (Max)	15 sec
Data Frame Duration	3 sec
Handover Retry Wait Time	15 sec
Simulation Duration	1000 sec
Rate of data occurrence per second	1 %
Sensor Node Location	Random

FIGURE 13. Simulation parameters for node mobility test and collision rate test.

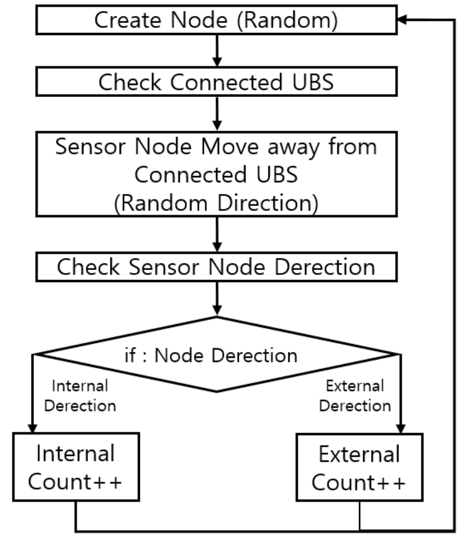

FIGURE 14. Algorithm-based flow chart for simulations of node mobility.

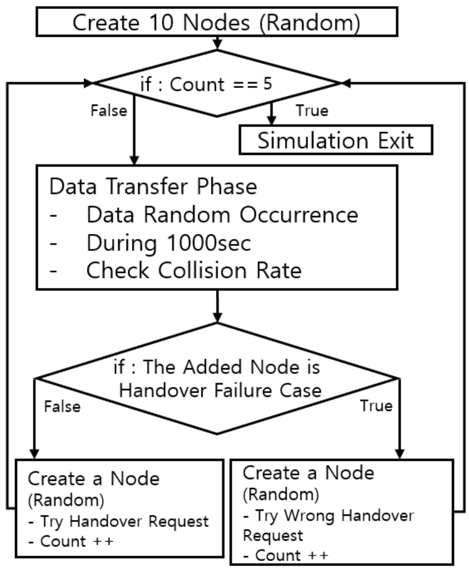

FIGURE 15. Flow chart for collision test.

the connected base station. For the verification, the simulation was conducted for 10,000 times in each case. For the calculation of network crashes of handover failure, the experiment was done by adding a node trying handover. It was done for 1,000 seconds, and each node has 1% of data transmission probability at every second. In the case that handover target is correctly predicted, even if the delivery for handover request message fails due to a crash, the handover can possibly be succeeded within the retransmission limit.

In the other case that handover target is not correct, we choose the method that repeats handover attempts for the number of retransmission limit. Fig. 15 shows the flow chart to the simulations.

VI. RESULT AND DISCUSSIONS

A. CASE. 1: CANDIDATE UBS COUNT IS 1

Fig. 16 shows the results for two methods. The simulations were repeated 10,000 times for the sensor node that moved away from the connected base station in Case 1 for both the UCC and UDSS methods. For the UCC method, the probability that the sensor nodes head to external UBSs is 76.38%, while the probability that the sensor nodes headed to internal UBSs is 23.62%.

In the case of the UDSS method, the trend is similar to the UCC method. 71.3% of the sensor nodes moved in the direction of the external UBSs while the remaining 28.7% moved in the direction of the internal UBSs. Most of the sensor nodes headed towards external UBSs.

B. CASE. 2: CANDIDATE UBS COUNT IS 2

Situations were considered in which the sensor nodes were located randomly in region ②, and each simulation was conducted 10,000 times. Fig. 16 shows the results of the

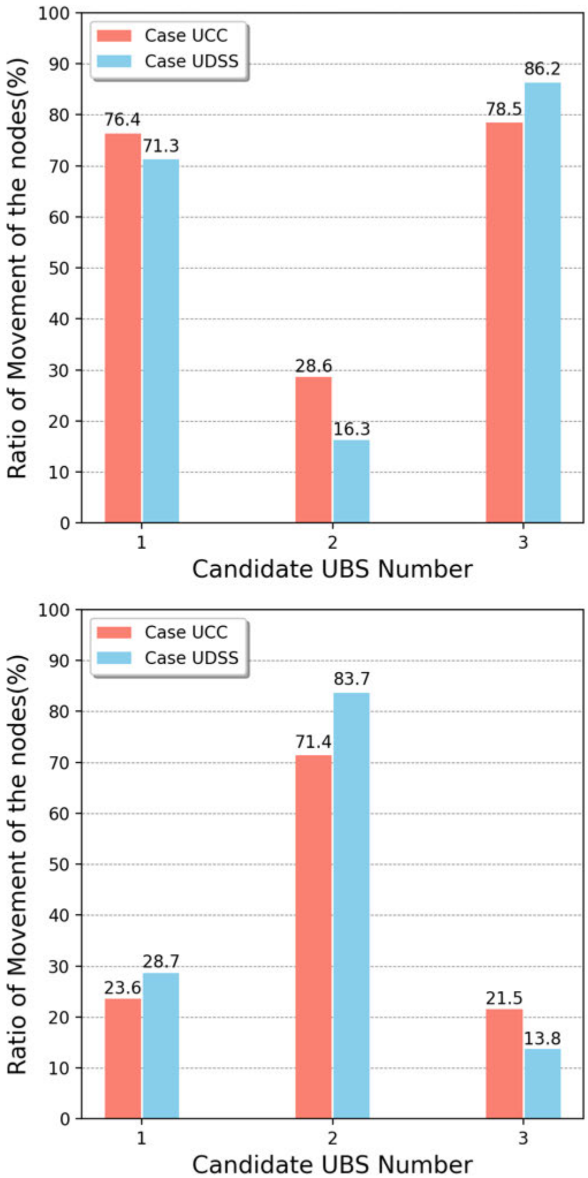

FIGURE 16. The simulation results for UCC and UDSS methods.

simulations, and indicates that the sensor nodes are most likely to head towards the internal UBSs in both the UCC method and the UDSS method. In the UDSS method, 83.7% of the nodes headed to the internal UBSs.

C. CASE. 3: CANDIDATE UBS COUNT IS 3

In case 3, situations were considered where the sensor nodes are randomly located in region ③, and each simulation was conducted 10,000 times. Fig. 16 shows the results of the simulations, and in the UCC case, the sensor nodes moved to the internal UBS with the second strongest signal with a probability of 78.47%. In UDSS, the sensor nodes moved to the internal UBS with the second strongest signal with a probability of 86.25% as expected.

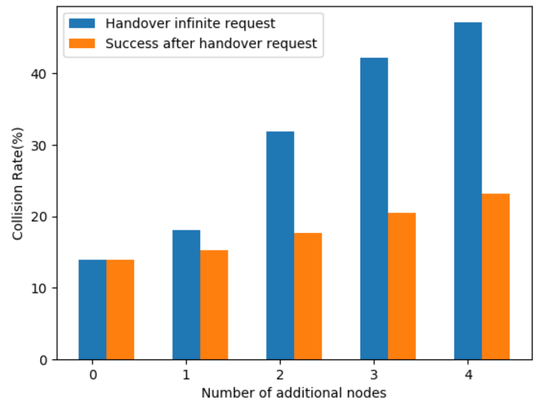

FIGURE 17. Network impact on IoUT networks in terms of collision rate according to the number of nodes.

D. NETWORK IMPACT: COLLISION TEST

Fig. 17 indicates the impact of the handover attempts on the IoUT networks of correct or incorrect prediction. In these simulations, we assumed that 10 sensor nodes are located in a single UBS cell, and these nodes are sending data based on a CSMA (Carrier Sense Multiple Access)-based random access mechanism to the UBS. In this experiment, we measured the packet collision rate for 1000 seconds of transmission. In Fig. 17, the number of additional nodes on the x-axis indicates the number of nodes that were added and attempted handover. This was done by adding sensor nodes one-by-one starting with 10 nodes communicating in a normal situation. The added sensor nodes requested handover until they succeed, and if a collision occurred they made requests again. If the handover was undertaken correctly, the sensor node started data transmission like other sensor nodes. As the number of added sensor nodes increased, we observe that the collision rate also increased. The orange-coloured bar shows the case where the added sensor nodes correctly predicted the handover target using the proposed methods. The blue-coloured bar indicates the case where the handover was attempted randomly, such that the handover request might fail in some cases. The handover procedure is repeated until it succeeds. The blue-coloured bar shows a steeper increase in the number of collisions. We thus note that the network performance can be increased by using the proposed handover prediction methods in terms of collision rate. When the prediction is correct, the collision rate is increased much less than the case in which the prediction is incorrect. The collision rates increase as 13.95%, 18.06%, 31.83%, 42.15%, and 47.11%, depending on the number of additional nodes. On the other hand, when the handover target cell is predicted correctly using the proposed methods, the collision rates are 13.92%, 15.35%, 17.68%, 20.54%, and 23.16%, depending on the number of additional nodes.

VII. CONCLUSION AND FUTURE WORK

In this paper, intelligent handover prediction schemes with zero scanning are proposed for reducing the battery power consumption and to increase the efficiency of IoUT networks. These are essential features of underwater IoT devices where battery life is limited. Based on the proposed handover prediction scheme, the power consumption can be reduced because channel scanning is not required. In addition, it is possible to improve the network efficiency by reducing the collision rate and by predicting the correct handover target cell. In this study, we considered a practical underwater IoT network under development for commercialization in South Korea. For further studies, the main idea of the proposed schemes is expected to also be applicable for practical IoT devices and systems in general.

REFERENCES

[1] I. F. Akyildiz, W. Su, Y. Sankarasubramaniam, and E. Cayirci, "A survey on sensor networks," *IEEE Commun. Mag.*, vol. 40, no. 8, pp. 102–114, Aug. 2002.

[2] C.-Y. Chong and S. P. Kumar, "Sensor networks: Evolution, opportunities, and challenges," *Proc. IEEE*, vol. 91, no. 8, pp. 1247–1256, Aug. 2003.

[3] E. M. Sozer, M. Stojanovic, and J. G. Proakis, "Underwater acoustic networks," *IEEE J. Ocean. Eng.*, vol. 25, no. 1, pp. 72–83, Jan. 2000.

[4] J. Heidemann, W. Ye, J. Wills, A. Syed, and Y. Li, "Research challenges and applications for underwater sensor networking," in *Proc. WCNC*, Las Vegas, NV, USA, 2006, pp. 228–235.

[5] M. Erol-Kantarci, H. T. Mouftah, and S. Oktug, "A survey of architectures and localization techniques for underwater acoustic sensor networks," *IEEE Commun. Surveys Tuts.*, vol. 13, no. 3, pp. 487–502, 3rd Quart., 2011.

[6] A. Davis and H. Chang, "Underwater wireless sensor networks," in *Proc. Oceans*, Hampton Roads, VA, USA, 2012, pp. 1–5.

[7] J.-H. Cui, J. Kong, M. Gerla, and S. Zhou, "The challenges of building mobile underwater wireless networks for Aquatic applications," *IEEE Netw.*, vol. 20, no. 3, pp. 12–18, May/Jun. 2006.

[8] Z. Zhu, Z. Wu, Z. Deng, H. Qin, and X. Wang, "An ocean bottom flying node AUV for seismic observations," in *Proc. AUV*, Porto, Portugal, 2018, pp. 1–5.

[9] C. C. Eriksen, T. J. Osse, R. D. Light, T. Wen, T. W. Lehman, P. L. Sabin, J. W. Ballard, and A. M. Chiodi, "Seaglider: A long-range autonomous underwater vehicle for oceanographic research," *IEEE J. Ocean. Eng.*, vol. 26, no. 4, pp. 424–436, Oct. 2001.

[10] L. Paull, S. Saeedi, M. Seto, and H. Li, "AUV navigation and localization: A review," *IEEE J. Ocean. Eng.*, vol. 39, no. 1, pp. 131–149, Jan. 2014.

[11] M. Gudmundson, "Analysis of handover algorithms (microcellular radio)," in *Proc. 41st IEEE Veh. Technol. Conf.*, 2011, pp. 537–542.

[12] M. E. Anagnostou and G. C. Manos, "Handover related performance of mobile communication networks," in *Proc. VTC*, Stockholm, Sweden, 1994, pp. 111–114.

[13] M. Stojanovic and J. Preisig, "Underwater acoustic communication channels: Propagation models and statistical characterization," *IEEE Commun. Mag.*, vol. 47, no. 1, pp. 84–89, Jan. 2009.

[14] K. Chen, M. Ma, E. Cheng, F. Yuan, and W. Su, "A survey on MAC protocols for underwater wireless sensor networks," *IEEE Commun. Surveys Tuts.*, vol. 16, no. 3, pp. 1433–1447, 3rd Quart., 2014.

[15] P. A. van Walree, "Propagation and scattering effects in underwater acoustic communication channels," *IEEE J. Ocean. Eng.*, vol. 38, no. 4, pp. 614–631, Oct. 2013.

[16] M. Molins and M. Stojanovic, "Slotted FAMA: a MAC protocol for underwater acoustic networks," in *Proc. Asia Pacific*, Singapore, 2006, pp. 1–7.

[17] F. A. Alfouzan, A. Shahrabi, S. M. Ghoreyshi, and T. Boutaleb, "An energy-conserving collision-free MAC protocol for underwater sensor networks," *IEEE Access*, vol. 7, pp. 27155–27171, 2019.

[18] A. A. Aziz, Y. A. Sekercioglu, P. Fitzpatrick, and M. Ivanovich, "A survey on distributed topology control techniques for extending the lifetime of battery powered wireless sensor networks," *IEEE Commun. Surveys Tuts.*, vol. 15, no. 1, pp. 121–144, Feb. 2013.

[19] D. Pompili, T. Melodia, and I. F. Akyildiz, "A CDMA-based medium access control for UnderWater acoustic sensor networks," *IEEE Trans. Wireless Commun.*, vol. 8, no. 4, pp. 1899–1909, Apr. 2009.

[20] M. Kyoung Park and V. Rodoplu, "UWAN-MAC: An energy-efficient MAC protocol for underwater acoustic wireless sensor networks," *IEEE J. Ocean. Eng.*, vol. 32, no. 3, pp. 710–720, Jul. 2007.

[21] S. Yoon and C. Qiao, "Cooperative search and survey using autonomous underwater vehicles (AUVs)," *IEEE Trans. Parallel Distrib. Syst.*, vol. 22, no. 3, pp. 364–379, Mar. 2011.

[22] N. Harsamizadeh Tehrani, M. Heidari, Y. Zakeri, and J. Ghaisari, "Development, depth control and stability analysis of an underwater remotely operated vehicle (ROV)," in *Proc. IEEE ICCA*, Xiamen, China, Jun. 2010, pp. 814–819.

[23] G. Meinecke, V. Ratmeyer, and J. Renken, "HYBRID-ROV–development of a new underwater vehicle for high-risk areas," in *Proc. OCEANS MTS/IEEE KONA*, Waikoloa, HI, USA, Sep. 2011, pp. 1–6.

[24] H. W. Kim and T. H. Im and H. S. Cho, "UCMAC: A cooperative MAC protocol for underwater wireless sensor networks," *Sensors*, vol. 18, no. 6, p. 1969, 2019.

[25] Y. Zhang, J. Li, Y. V. Zakharov, J. Li, Y. Li, C. Lin, and X. Li, "Deep learning based single carrier communications over time-varying underwater acoustic channel," *IEEE Access*, vol. 7, pp. 38420–38430, 2019.

[26] R. Jiang, X. Wang, S. Cao, J. Zhao, and X. Li, "Deep neural networks for channel estimation in underwater acoustic OFDM systems," *IEEE Access*, vol. 7, pp. 23579–23594, 2019.

[27] Q. Guan, F. Ji, Y. Liu, H. Yu, and W. Chen, "Distance-vector-based opportunistic routing for underwater acoustic sensor networks," *IEEE Internet Things J.*, vol. 6, no. 2, pp. 3831–3839, Apr. 2019.

[28] D. Shin and D. Kim, "A dynamic NAV determination protocol in 802.11 based underwater networks," in *Proc. IEEE Int. Symp. Wireless Commun. Syst.*, 2008, pp. 401–405.

[29] S. Park and O. Jo, "Q-NAV: NAV setting method based on reinforcement learning in underwater wireless networks," *J. Converg. Inf. Technol.*, vol. 10, no. 6, pp. 1–7, 2020, doi: 10.22156/CS4SMB.2020.10.06.001.

[30] K. P. Hunt, J. J. Niemeier, and A. Kruger, "RF communications in underwater wireless sensor networks," in *Proc. IEEE Int. Conf. Electro/Information Technol.*, Normal, IL, USA, May 2010, pp. 1–6.

[31] B. Kelley, K. Manoj, and M. Jamshidi, "Broadband RF communications in underwater environments using multi-carrier modulation," in *Proc. IEEE Int. Conf. Syst., Man Cybern.*, San Antonio, TX, USA, Oct. 2009, pp. 2303–2308.

[32] J. Shi, S. Zhang, and C. Yang, "High frequency RF based non-contact underwater communication," in *Proc. Oceans*, Yeosu, China, 2012, pp. 1–6.

[33] C. T. Geldard, J. Thompson, and W. O. Popoola, "An overview of underwater optical wireless channel modelling techniques : (Invited Paper)," in *Proc. Int. Symp. Electron. Smart Devices (ISESD)*, Badung-Bali, IN, USA, Oct. 2019, pp. 1–4.

[34] J. Huang, G. Wen, J. Dai, L. Zhang, and J. Wang, "Channel model and performance analysis of long-range deep sea wireless photon-counting communication," *Opt. Commun.*, vol. 473, Oct. 2020, Art. no. 125989, doi: 10.1016/j.optcom.2020.125989.

[35] B. Li, S. Zhou, M. Stojanovic, L. Freitag, and P. Willett, "Multicarrier communication over underwater acoustic channels with nonuniform Doppler shifts," *IEEE J. Ocean. Eng.*, vol. 33, no. 2, pp. 198–209, Apr. 2008.

[36] M. Zorzi, P. Casari, N. Baldo, and A. Harris, "Energy-efficient routing schemes for underwater acoustic networks," *IEEE J. Sel. Areas Commun.*, vol. 26, no. 9, pp. 1754–1766, Dec. 2008.

[37] H.-J. Son, J.-I. Kang, T. Q. Minh Nhat, S. K. Kim, and H.-S. Choi, "Study on underwater optical communication system for video transmission," *J. Ocean Eng. Technol.*, vol. 32, no. 2, pp. 143–150, Apr. 2018, doi: 10.26748/KSOE.2018.4.32.2.143.

[38] S. Park, J. Byun, K.-S. Shin, and O. Jo, "Ocean current prediction based on machine learning for deciding handover priority in underwater wireless sensor networks," in *Proc. Int. Conf. Artif. Intell. Inf. Commun. (ICAIIC)*, Fukuoka, Japan, Feb. 2020, pp. 505–509.

[39] N. K. Sinai, J. Namgung, S. Y. shin, and S. Park, "Handover protocol in ad-hoc diver networks using visual light communication," in *Proc. ICUFN*, Zagreb, Croatia, 2019, pp. 604–609.

[40] H. Y. Hwang and H.-S. Cho, "Throughput and delay analysis of an underwater CSMA/CA protocol with multi-RTS and multi-DATA receptions," *Int. J. Distrib. Sensor Netw.*, vol. 12, no. 5, May 2016, Art. no. 2086279, doi: 10.1155/2016/2086279.

[41] C. Yun, J.-W. Park, and S. Choi, "Backhaul resource allocation protocol for underwater cellular communication networks," *J. Korean Inst. Commun. Inf. Sci.*, vol. 42, no. 2, pp. 393–402, Feb. 2017, doi: 10.7840/kics.2017.42.2.393.

[42] H. G. Kim and H.-S. Cho, "A sensor-node searching scheme for initial cell configuration in underwater cellular network," *J. Korean Inst. Commun. Inf. Sci.*, vol. 44, no. 1, pp. 68–71, Jan. 2019, doi: 10.7840/kics.2019.44.1.68.

[43] I. Ahmad and K. Chang, "Design of system-level simulator architecture for underwater acoustic communications and networking," in *Proc. Int. Conf. Inf. Commun. Technol. Converg. (ICTC)*, Jeju, South Korea, Oct. 2016, pp. 384–386.

[44] R. Pec, M. Khan, M. Asim, and Y. Cho, "Random access for underwater acoustic cellular systems," *Sensors*, vol. 18, no. 2, p. 432, Feb. 2018, doi: 10.3390/s18020432.

[45] S. Park and O. Jo, "Probabilistic priority handover in underwater IoT networks," in *Proc. KICS*, Jeju, South Korea, 2019, pp. 590–591.

[46] J. Byun, Y. Cho, T. Im, H. Ko, K. Shin, and O. Jo, "Iterative learning for reliable underwater link adaptation," in *Proc. AAAI*, New York, NY, USA, 2020, pp. 13761–13762.

[47] M.-S. Kim, T.-S. Lee, J.-H. Kim, T.-H. Im, and H.-L. Ko, "Performance analysis of FMT-OFDM system in the underwater channel environment," in *Proc. OCEANS*, Shanghai, China, Apr. 2016, pp. 1–4.

[48] M.-S. Kim, T.-H. Im, Y.-H. Cho, K.-W. Kim, and H.-L. Ko, "HFM design for timing synchronization in underwater communications systems," in *Proc. OCEANS*, Aberdeen, UK, Jun. 2017, pp. 1–4.

SEOKHYEON PARK received the bachelor's degree from the Department of Computer Science, Semyung University, Jecheon, South Korea, in 2019. He is currently pursuing the master's degree with the Department of Computer Science, Chungbuk National University, Cheongju, South Korea. His research interests include underwater communications, machine learning, network protocols, and the Internet of Things.

OHYUN JO (Member, IEEE) received the B.S., M.S., and Ph.D. degrees in electrical engineering from the Korea Advanced Institute of Science and Technology (KAIST), in 2005, 2007, and 2011, respectively. From April 2011 to February 2016, he was with Samsung Electronics in charge of research and development for future wireless communication systems, applications, and services. From March 2016 to July 2017, he was a Senior Researcher with the Electronics and Telecommunications Research Institute (ETRI). From August 2017 to February 2018, he was an Associate Professor with the Department of Electrical Engineering. He is currently an Associate Professor with the Department of Computer Science, Chungbuk National University. He has authored or coauthored more than 60 articles. He holds more than 160 registered and filed patents. His research interests include millimeter-wave communications, next-generation WLAN/WPAN systems, 5G mobile communication systems, military communications, the Internet of Things, future wireless solutions/applications/services, machine learning, and embedded communications ASIC design. He was a recipient of numerous recognitions, including the Gold Prize in Samsung Annual Award, the Most Creative Researcher of the Year Award, the Best Mentoring Award, the Major Research and Development Achievement Award, and the Best Improvement of Organization Culture Award.